Title: Distinct branches of the N-end rule pathway modulate the plant immune response

Authors:

Jorge Vicente[1]*, Guillermina M. Mendiondo[1], Jarne Pauwels[2,9], Victoria Pastor[3], Yovanny Izquierdo[4], Christin Naumann[5], Mahsa Movahedi[8b], Daniel Rooney[1], Daniel J. Gibbs[1a], Katherine Smart[6], Andreas Bachmair[7], Julie E Gray[8], Nico Dissmeyer[5], Carmen Castresana[4], Rumiana V. Ray[1], Kris Gevaert[2,9], Michael J. Holdsworth[1]*

Author affiliations:

[1]School of Biosciences, University of Nottingham, LE12 5RD, UK
[2]VIB-UGent Center for Medical Biotechnology Albert Baertsoenkaai 3, B-9000 Ghent, Belgium
[3]Área de Fisiología Vegetal, Departamento de Ciencias Agrarias y del Medio Natural, Universitat Jaume I, Castellón, Spain
[4]Centro National de Biotecnología CSIC, C/ Darwin, 3, Campus of Cantoblanco E-28049 Madrid, Spain
[5]Leibniz Institute of Plant Biochemistry (IPB), Weinberg 3 D-06120 Halle (Saale), Germany and ScienceCampus Halle – Plant-Based Bioeconomy, Halle (Saale), Germany
[6]SABMiller plc. SABMiller House, Church Street West, Woking, Surrey, GU21 6HS, UK
[7]Dept. of Biochemistry and Cell Biology, Max F. Perutz Laboratories, University of Vienna, Dr. Bohr Gasse 9, Vienna A-1030, Austria
[8]Department of Molecular Biology and Biotechnology, University of Sheffield, Sheffield S10 2TN, United Kingdom
[9]Department of Biochemistry, Ghent University, Albert Baertsoenkaai 3, B-9000 Ghent, Belgium

Current Address: [a]School of Biosciences, University of Birmingham, Edgbaston, B15 2TT, UK; [b]Department of Biosciences, Durham University, Stockton Road, Durham, DH1 3LE

Corresponding authors:

Michael Holdsworth and Jorge Vicente, School of Biosciences, University of Nottingham, LE12 5RD, UK.
Tel: 00441159516046,
Emails:
michael.holdsworth@nottingham.ac.uk; Jorge.Vicente_Conde@nottingham.ac.uk

Correspondence and material requests should be addressed to Professor Michael Holdsworth, School of Biosciences, University of Nottingham, LE12 5RD, UK. 00441159516046, michael.holdsworth@nottingham.ac.uk

Summary

- The N-end rule pathway is a highly-conserved constituent of the ubiquitin proteasome system, yet little is known about its biological roles.

- Here we explored the role of the N-end rule pathway in the plant immune response. We investigated the genetic influences of components of the pathway and known protein substrates on physiological, biochemical and metabolic responses to pathogen infection.

- We show that the glutamine (Gln) deamidation and cysteine (Cys) oxidation branches are both components of the plant immune system, through the E3 ligase PROTEOLYSIS (PRT)6. In *Arabidopsis thaliana* Gln-specific amino-terminal (Nt)-amidase (NTAQ1) controls expression of specific defence-response genes, activates the synthesis pathway for the phytoalexin camalexin and influences basal resistance to the hemibiotroph pathogen *Pseudomonas syringae* pv *tomato* (*Pst*). The Nt-Cys ETHYLENE RESPONSE FACTOR VII transcription factor substrates enhance pathogen-induced stomatal closure. Transgenic barley with reduced *HvPRT6* expression showed enhanced resistance to *Ps japonica* and *Blumeria graminis* f. sp. *hordei*, indicating a conserved role of the pathway.

- We propose that that separate branches of the N-end rule pathway act as distinct components of the plant immune response in flowering plants.

Key words:

Amino-terminal glutamine amidase

Group VII Ethylene Response Factor transcription factor

N-end rule pathway

Plant immunity

Proteostasis

Introduction:

The regulation of protein stability through the Ubiquitin Proteasome System (UPS) is a central component of cellular homeostasis, environment interactions and developmental programmes (Varshavsky, 2012), and an important component of the plant immune system (Zhou & Zeng, 2017). Plants have evolved to recognize the presence of a pathogen in two main ways. Basal (primary) defence is characterised by the recognition of pathogen elicitors called Pathogen Associated Molecular Patterns (PAMPs) by protein receptors known as Pattern Recognition Receptors (PRR), activating PAMP-Triggered Immunity (PTI) (Boller & Felix, 2009). When this response is effective, pathogens can deliver effector molecules into the host cells to weaken PTI and facilitate infection triggering a second layer of defence (Effector Triggered Immunity; ETI). ETI is typically a qualitative response based on interference with pathogen effector activity by plant resistance (R) gene products, localized inside the cell (Dangl & Jones, 2001). Both PTI and ETI induce similar immune responses but of different amplitude, with ETI often resulting in a hypersensitive response (HR). The specific set of mechanisms activated also depend to a large extent on the life strategy of the pathogen and how adapted they are to the host. Typically, the plant hormones jasmonic acid (JA) and ethylene (ET) mediate responses to non-adapted necrotrophs that cause host cell death to acquire nutrients from dead or senescent tissues (Grant & Jones, 2009; Pieterse *et al.*, 2009) whilst salicylic acid (SA) plays a crucial role in activating defence against adapted biotrophs and hemibiotrophs. Recently, regulation of protein stability by the Arg/N-end rule pathway of ubiquitin-mediated proteolysis has been demonstrated to play a role in plant responses to biotic stress. The pathway is associated with increased development of clubroot caused by the obligate biotroph *Plasmodiophora brassicae* (Gravot *et al.*, 2016). Induction of components of the hypoxia response, controlled by Group VII ETHYLENE RESPONSE FACTOR (ERFVII) transcription factor substrates (ERFVIIs), enhanced clubroot development, indicating that the protist hijacks the N-end rule ERFVII regulation system to enhance infection. In another study, inactivation of different components of the Arg/N-end rule pathway was shown to result in greater susceptibility of Arabidopsis to necrotrophic pathogens and altered timing and amplitude of response to the hemibiotroph *Pseudomonas syringae* pathovar *tomato* (*Pst*) AvrRpm1 (de Marchi *et al.*, 2016). A correlation between Nt-Acetylation and the stability of a Nod-like receptor, Suppressor of NPR1, Constitutive 1 (SNC1) was also reported (Xu *et al.*, 2015). Whilst these reports provide evidence that the N-end rule pathway is involved in the regulation of plant defence responses, the mechanisms,

substrates or their function in resistance have not been investigated previously (Gibbs *et al.*, 2014a). The N-end rule pathway of ubiquitin-mediated proteolysis is an ancient and conserved branch of the UPS (Gibbs *et al.*, 2014a). This pathway relates the half-life of substrates to the amino terminal (Nt-) residue, which forms part of an N-degron (Gibbs *et al.*, 2014a). Destabilizing residues of the Arg/N-end rule are produced following endo-peptidase cleavage and may be primary, secondary or tertiary (Figure 1A). Basic and hydrophobic primary destabilizing residues are recognized directly by N-recognin E3 ligases, in plants represented by two proteins, PROTEOLYSIS(PRT)6 and PRT1 (Gibbs *et al.*, 2014a). Secondary destabilizing residues (Glu, Asp and oxidized Cys) can be N-terminally arginylated by arginyl-transferases (ATEs), and tertiary destabilizing residues (Gln, Asn and Cys) can undergo modifications to form secondary destabilizing residues (Gibbs *et al.*, 2014a). Oxidation of Cys was shown in vitro to occur both non-enzymically (Hu *et al.*, 2005) or enzymatically (Weits *et al.*, 2014; White *et al.*, 2017), whereas in higher eukaryotes deamidations of Gln and Asn are carried out by residue-specific N-terminal amidases (NTAQ1 (Wang *et al.*, 2009) and NTAN1 (Grigoryev *et al.*, 1996) respectively). This hierarchical structure is conserved in eukaryotes, and physiological substrates with N-terminal residues representing these destabilizing classes have been identified (Piatkov *et al.*, 2014). The Usp1 deubiquitylase is targeted for degradation through the de-amidation branch of the Arg/N-end rule via NTAQ1 as a consequence of auto-cleavage, that reveals N-terminal Gln (Piatkov *et al.*, 2012). Proteins with similarities to mouse NTAN1 and NTAQ1 are encoded in higher plant genomes, in Arabidopsis by AT2G44420 (putative NTAN1) and AT2G41760 (putative NTAQ1). Expression of these in a de-amidation deficient *nta1* mutant of *Saccharomyces cerevisiae* could functionally restore degradation of the N-end rule reporters Asn-β−galactosidase (β−Gal) and Gln-β-Gal, respectively. ATE activity was required for this destabilization in yeast (Graciet *et al.*, 2010). Although the Arg/N-end rule pathway is evolutionarily highly conserved in eukaryotes, few substrates or functions for different branches have been shown. In plants the Cys branch of the Arg/N-end rule pathway controls homeostatic response to hypoxia (low oxygen) and NO sensing through the Met-Cys initiating ERFVII transcription factor substrates (Gibbs *et al.*, 2011; Licausi *et al.*, 2011; Gibbs *et al.*, 2014b).

In this paper, we investigated the role of distinct branches of the Arg/N-end rule pathway in the immune response in Arabidopsis and barley (*Hordeum vulgare*). We demonstrate that two branches of the pathway, Glu- deamidation and Cys-oxidation, regulate resistance to the hemibiotroph *Pst* and the biotroph *Blumeria*

157 *graminis* f. sp. *hordei* (*Bgh*). We also show a significant role for Gln de-amidase
158 NTAQ1 in the regulation of molecular components associated with basal responses
159 to infection, and a role for both NTAQ1 and the known Nt-Cys ERFVII substrates in
160 resistance related to stomatal function.
161

Materials and Methods:

Plant material, growth conditions and experimental design

Arabidopsis thaliana seeds were obtained from NASC, UK unless otherwise stated, including *prt6-1* (SAIL 1278_H11), *ntaq1-1* (SALK_075466). Mutant *ntan1-1* (Q202* mutation [CAA to TAA]) was obtained from the Seattle TILLING project (http://tilling.fhcrc.org). Mutant *ntaq1-3* was obtained from the GABI-Kat T-DNA insertion collection (GK_306F08). The *pad3-1* null allele was described previously (Glazebrook & Ausubel, 1994). Mutants are in the Col-0 (Wild Type, WT) accession. Plants were grown and assays performed in controlled-environment rooms under the following conditions: 12 h of light (23°C) and 12 h of dark (18°C), 60-70% relative humidity. Plants were treated between 3 and 4 weeks after germination. Barley plant genotypes and growth conditions were as previously described (Mendiondo *et al.*, 2016).

Construction of transgenic Arabidopsis lines ectopically-expressing NTAQ1

To generate Arabidopsis NTAQ1 overexpressing lines, full-length cDNA sequence (with and without the STOP codon) was amplified from 7 day old seedling cDNA and recombined into pDONR221. The constructs were mobilized into pH7m34G and pH7m24GW2, with the GSrhino tag in C-terminal or N-terminal position of the NTAQ1, respectively (Karimi *et al.*, 2007). Then the constructs were transformed into *Agrobacterium tumefaciens* (strain GV3101 pMP90) and Arabidopsis *ntaq1-3* using standard protocols (Clough & Bent, 1998).

In vitro assay for NTAQ1 activity.

The Arabidopsis NTAQ1 coding sequence was cloned from cDNA and flanked by an N-terminal tobacco etch virus (TEV) protease recognition sequence (ENLYFQ-X) using primers ss_ntaq1_tev and as_ntaq1_gw, followed by a second PCR with as_ntaq1_gw and adapter tev attaching a Gateway attB1 site for sub-cloning into pDONR201 (Invitrogen). An LR reaction into pVP16 (Thao *et al.*, 2005) leads to an N-terminal 8xHis:MBP double affinity tag. Assay for NTAQ activity was performed as described previously (Wang *et al.*, 2009) with slight modifications. The assay was performed in three technical replicates from three independent NTAQ1 protein expressions. The activity of NTAQ1 towards QKGSGAW was used as 100% reference value.

Analysis of pathogen growth in plant material

The bacterial suspension was or injected with a needleless syringe into the abaxial side of leaves or sprayed on the surface of the leaves of 3.5-week-old plants. *Pst* DC3000 *avrRpm1* and *Pst* DC3000 were grown overnight at 28°C in Petri plates with King's B medium. For analysis of bacterial growth, three leaves per plant of at least 7 plants were injected with a bacterial suspension of 10^6 cfu/ml ($O.D._{600nm}$ 0.1= 10^8 cfu ml^{-1}) or sprayed with a suspension of 10^8 cfu/ml. A disc of 0.28 cm^2 from each infected leaf was excised at 96 h, pooled in triplicate, homogenized, diluted and plated for counting. The inoculation of *Botrytis cinerea* was performed by pipetting a drop of 10 µl of a suspension of $5x10^5$ spores/ml to the surface of the leaves. The response was analyzed by measuring the diameter of the symptoms produced in three leaves of at least 20 independent plants.

Barley plants were infected with *Fusarium* and *Blumeria* as previously described (Ajigboye *et al.*, 2016). Leaf material of twenty five day old Barley plants (grown under controlled conditions (20°C/15 °C; 16-h photoperiod; 80% RH, 500 µmol/m^2/s metal halide lamps (HQI) supplemented with tungsten bulbs)) were syringe infiltrated with 0.1 OD *Ps pv japonica* (obtained from the NCPPB (National Collection of Plant Pathogenic Bacteria), UK. Leaf material was collected before treatment and 4 days after inoculation for conductivity assays and RNA extraction. Production of H_2O_2 was visualized by staining with 3,3'-diaminobenzidine tetrachloride as described (Thordal-Christensen *et al.*, 1997; Moreno *et al.*, 2005).

Stomatal aperture analyses

For stomatal aperture in response to *Pst* assays leaves from 3.5 week-old plants were used. In the morning after two hours the lights switch on, peels from abaxial side of leaves were placed in Petri dishes containing 10 mM MES/KOH pH 6.1, 50 mM KCl and 0.1 mM $CaCl_2$ for 2h in continuous light. Then the buffer was replaced for a solution of *Pst* DC3000 (O.D. 0.2: $2x10^8$ cfu/ml). Stomatal aperture was measured after 0, 1 and 3h of incubation with the bacteria. Stomatal aperture measurements for ABA sensitivity assays were carried out on detached leaf epidermis as described previously (McAinsh *et al.*, 1991; Chater *et al.*, 2011).

Protein extraction and Immunoblotting

Protein extractions and immunoblotting were carried out as described previously (Gibbs *et al.*, 2011).

Gene expression analysis

RNA extraction, cDNA synthesis, semi- and quantitative RT-PCR were performed as previously described for Arabidopsis (Gibbs *et al.*, 2011; Gibbs *et al.*, 2014b) and barley (Mendiondo *et al.*, 2016). For primers used see Supplementary Table 4.

Analysis of nitrate reductase activity

Nitrate reductase was assayed as previously (Vicente *et al.*, 2017) with modifications described elsewhere (Kaiser & Lewis, 1984).

Analysis of protein, RNA and metabolites.

Protein extraction, immunoblotting and histochemistry were carried out as described previously (Gibbs *et al.*, 2011). Quantitative rt-PCR was performed as previously described for Arabidopsis (Gibbs *et al.*, 2014b) and barley (Mendiondo *et al.*, 2016). Proteomics (Vu *et al.*, 2016) and metabolomics (Gamir *et al.*, 2012; Sánchez-Bel *et al.*, 2018) analyses were carried out as previously described.

Experimental statistical analyses

All experiments were performed at least in triplicate. Statistical comparisons were conducted with GraphPad Prism 7.0 software. Horizontal lines represent standard error of the mean values in all graphs. For statistical comparisons we used Student's t-test, where statistically significant differences are reported as *** ($p < 0.001$), ** ($p < 0.01$), * ($p < 0.05$), and one way Analysis of Variance (ANOVA) with Tukey's multiple comparisons test, where significant differences (alpha< 0.05) are denoted with different letters.

Results:

Gln de-amidase and Cys oxidation branches of the Arg/N-end rule pathway increase basal resistance against *Pst* DC3000

The role for the Arg/N-end rule pathway in the plant immune response was assessed using the model bacterial pathogen *Pseudomonas syringae* pv *tomato* DC3000 and T-DNA insertion null mutants of the putative Gln-specific amino-terminal amidase NTAQ1 (AT2G41760) (Supporting Information Fig. S1a-d) and N-recognin E3 ligase PRT6 (AT5G02310) genes, and a premature termination allele of the putative Asn-specific amino-terminal amidase NTAN1 (AT2G44420) (Q202*) (Figure 1a). The entire effect of NTAQ1, NTAN1 and Cys- branches of the Arg/N-end rule pathway on response to pathogen challenge can be assessed by analysis of the *prt6* mutant, as this removes E3 ligase activity, thus stabilizing all substrates of NTAQ1, NTAN1 and substrates with Nt-Cys (Figure 1a). Bacterial growth in leaves of *prt6* was significantly lower by 4 days post infiltration with virulent (*Pst* DC3000) or avirulent (*Pst* DC3000 *avrRmp1*) strains, indicating that substrates destabilized by PRT6 action contribute to the immune response (Figure 1b, Supporting Information Fig. S2a). In comparison, *ntaq1* alleles also showed significantly lower bacterial growth (comparable to that of *prt6*) compared to both the *ntan1-1* mutant or the wild-type (WT) Col-0 for plants grown from seed in soil under neutral days (12h light, 12h dark). These results are opposite to those obtained by de Marchi *et al.* (de Marchi *et al.*, 2016), who found enhanced sensitivity to *Pst* DC3000 of N-end rule mutants *prt6* and *ate1 ate2* (that removes ATE Nt-arginylation activity, Figure 1a). To investigate this difference, we assayed bacterial growth under conditions used by de Marchi *et. al.* for plant growth and infection. In their case germination and initial 7 days growth of seedlings was carried out on agar containing MS media and 0.5% sucrose before transfer to soil, and following transfer plants were grown under short day conditions (9h light, 15h dark). We grew Col-0, *prt6-1* and *ate1 ate2* under these conditions and assayed bacterial growth 2 and 4 days post infiltration. As for plants grown under neutral days, we found that by 4 days post-infection, bacterial growth was significantly lower in N-end rule mutants than in WT (Supporting Information Fig. S2b). All subsequent reported experiments were carried out using plants grown from seed in neutral day conditions.

Tissue cellular leakage measured 4 days following infection was significantly lower in *prt6* and *ntaq1* mutants (Figure 1c, Supporting Information Fig. S1d). Expression in WT of *NTAQ1* and *PRT6* was not strongly affected by infection with either bacterial strain (Supporting Information Fig. 2c). Inoculation with the PTI

inducer *Pst* DC3000 *hrpA*$^-$ (with a compromised type-three secretion system), resulted in reduced susceptibility of *prt6* and *ntaq1* mutants compared to WT or *ntan1* (Figure 1d). Ectopic expression of either Nt- or C-terminally tagged NTAQ1 removed enhanced resistance of *ntaq1-3* (Figure 1e), and the double mutant *prt6-1 ntaq1-3* did not show significant difference compared with the single mutants *prt6-1* or *ntaq1-3* (Figure 1f). It was previously suggested that formation of N-terminal pyroglutamate by glutaminyl cyclase (GC) might compete with NTAQ1 for Nt-Gln substrates (Wang *et al.*, 2009), implying that a lack of GC activity could lead to enhanced susceptibility. We observed a similar response to *Pst* DC3000 of WT and a mutant of *GLUTAMINYL CYCLASE1* (*GC1*) (Schilling *et al.*, 2007) (Supporting Information Fig. S2d), indicating that competition for N-Gln substrates between NTAQ1 and GC1 is not relevant for the regulation of bacterial growth following infection. To define the biochemical action of NTAQ1, we analysed the Nt-deamidation capacity of recombinant Arabidopsis NTAQ1, that showed high specificity for Nt-Gln in comparison to Nt-Asn, -Gly and-Lys (Figure 1g).

Using mutants in which ERFVII activity was removed (Abbas *et al.*, 2015) (*rap2.12 rap2.2 rap2.3 hre1 hre2* pentuple mutant, hereafter *erfVII*, and the *prt6 erfVII* sextuple mutant), analysis of infections of *Pst* DC3000 following infiltration showed no significant influence of ERFVIIs in affecting apoplastic growth of either virulent or avirulent *Pst* strains (Figure 2a, Supporting Information Fig. S3a). Bacterial growth 4 days following foliar spray application of *Pst* DC3000 revealed greater resistance of both *prt6-1* and *ntaq1-3* mutants compared to WT or *ntan1-1* (Figure 2b, Supporting Information Fig. S3b), that for both foliar spray and injection required SA (analysed in double mutant combinations of *prt6-1* or *ntaq1-3* with *sid2-1*, SID2 is an isochorismate synthase required for SA synthesis (Nawrath & Metraux, 1999)) (Supporting Information Fig. S3c). Stomatal closure is a key component of early defence response following pathogen attack (Arnaud & Hwang, 2015). We found that in response to *Pst*, WT initially closed and then, induced by the pathogen, reopened stomata, as did *prt6-1* and *ntaq1-3*. The *erfVII* and *prt6 erfVII* mutants failed to close stomata at any point (Figure 2c). ERFVIIs have previously been shown to regulate stomatal ABA sensitivity via the N-end rule pathway (Vicente *et al.*, 2017), and we also found *ntaq1-3* stomata were hypersensitive to ABA (Supporting Information Fig. S3d). In response to *Pst* DC3000 infection following foliar spray application resistance was significantly lower in the absence of ERFVII transcription factors (either *erfVII* or *prt6 erfVII*) compared respectively to WT or *prt6* (Figure 2d). Response to foliar spray application of *Pst* DC3000 was associated with a large decrease in activity and expression of NITRATE REDUCTASE (NR) (Figure 2e,f), a

reduction previously linked with increased basal resistance against *Pst* (Park *et al.*, 2011), whereas expression of *ADH1*, a marker for hypoxia, was only increased immediately following pathogen challenge (Supporting Information Fig. S3e). Infection with *Pst* DC3000 was associated by 24h with increased stabilization of an artificial Cys-Arg/N-end rule substrate derived from the construct *35S:MC-^{HA}GUS*, that following constitutive MetAP activity is expressed as C-^{HA}GUS (Gibbs *et al.*, 2014b; Vicente *et al.*, 2017) (Figure 2g). To clarify whether plant-derived factors were solely responsible for the control of the stability of C-^{HA}GUS, we injected the PAMP peptide flg22, and showed that injection of flg22 was able to stabilize C-^{HA}GUS (Figure 2h).

The Arg/N-end end rule pathway has a conserved function in the immune response

To determine the conservation of Arg/N-end rule pathway role in the immune response, we tested responses to pathogens in barley, a monocot species distantly related to Arabidopsis, in which the expression of the *PRT6* orthologue gene *HvPRT6* was reduced by RNAi (Mendiondo *et al.*, 2016). Following inoculation with a strain of *Pseudomonas syringae* pv *japonica* with known pathogenicity to barley (Dey *et al.*, 2014), significantly lower bacterial load was observed in *HvPRT6* RNAi leaves compared to the WT (Figure 3a). Similarly, *HvPRT6* RNAi plants exhibited reduced development and severity of mildew caused by *Bgh* (Figure 3b,c). In contrast, susceptibility of *HvPRT6* RNAi to the necrotrophic fungi *Fusarium graminearum* or *F. culmorum*, tested on detached leaves was increased compared to the WT (Figure 3d). To assess the response of *prt6-1* in Arabidopsis to a necrotroph we inoculated the mutant and WT with the fungal pathogen *Botrytis cinerea* but we failed to observe any significant differences in disease severity, measured as diameter of necrotic lesions (Supporting Information Fig. S3f). Infection of barley with *Ps* pv *japonica* or *Bgh* also resulted in accumulation of the artificial Nt-Cys substrate CGGAIL-GUS (from *pUBI:MCGGAIL-GUS*, containing the first highly conserved seven residues of ERFVIIs (Gibbs *et al.*, 2014b; Mendiondo *et al.*, 2016; Vicente *et al.*, 2017)), therefore Nt-Cys stabilization in response to infection is conserved in flowering plants (Figure 3e).

NTAQ1 regulates expression of the camalexin biosynthesis pathway

A shotgun proteomic analysis of total proteins from untreated *ntaq1-3* and WT adult leaves revealed a total of 13 proteins which were significantly differentially regulated, 12 exhibited increased and one decreased abundance in *ntaq1-3* (Supplementary

Table1). The functions of most *ntaq1* upregulated proteins are related to oxidative, biotic and abiotic stresses, including a 2-OXOGLUTARATE OXYGENASE (AT3G19010) potentially involved in quercetin biosynthesis and targeted by bacterial effectors (Truman *et al.*, 2006) and DJ-1 protein homolog E (DJ1E) involved in response to PAMPs (Lehmeyer *et al.*, 2016). Not all *ntaq1* upregulated protein were also upregulated at the level of RNA (Supporting Information Fig. S4). Several *ntaq1* over-accumulated proteins are involved in the regulation of Reactive Oxygen Species (ROS). However, analysis of gene expression of a ROS accumulation marker, the antioxidant enzyme CATALASE1 (CAT1), and histochemical analysis of the accumulation of the ROS hydrogen peroxide (H_2O_2) during infections with *Pst* failed to reveal significant differences between the mutants *ntaq1* and *prt6* and WT (Supporting Information Fig. S5). Increased tolerance of the mutants which was associated with less cellular damage required SID2, an isochorismate synthase required for SA synthesis (Nawrath & Metraux, 1999)), as double mutant combinations of *prt6-1* or *ntaq1-3* with *sid2-1* showed susceptibility similar to the *sid2* single mutant (Supporting Information Fig. S3c). Analysis of phytohormone levels indicated that there were no differences between *ntaq1-3*, *prt6-1* or WT in untreated or infected leaves for SA, JA or IAA (Figure 4, Supporting Information Fig. S7). These results together suggest a functional redundancy of *ntaq1* up-regulated proteins with other antioxidant mechanisms, already documented in the case of the GLUTATHIONE S-TRANSFERASEs (GSTs) (Sappl *et al.*, 2009), or alternative roles for *ntaq1* up-regulated proteins in plant defense.

One of the identified proteins up-regulated in *ntaq1*, the phi class GSTF6, functions in secondary metabolism related to the synthesis of the major Arabidopsis phytoalexin, camalexin (Su *et al.*, 2011), as do the up-regulated proteins PUTATIVE ANTHRANILATE PHOSPHORIBOSYLTRANSFERASE (involved in the synthesis of the camalexin precursor tryptophan (Zhao & Last, 1996)) and IAA-AMINO ACID HYDROLASE (ILL4), that generates indole-3-acetic acid (IAA) from its conjugated form (Davies *et al.*, 1999). Another up-regulated protein, GSTF7 was hypothesized to play a role in camelaxin synthesis based on its induction in the constitutively active MKK9 mutant (Su *et al.*, 2011). Our analysis of previously published transcriptome data (de Marchi *et al.*, 2016) comparing gene expression in *ate1 ate2* with WT, and comparing gene expression during *Pst* infection in Col-0 and *ate1 ate2* also showed increased expression of RNAs encoding camalexin synthesis genes (Supplementary Tables 2,3). Analysis of transcript expression indicated greater accumulation for most genes of camalexin synthesis in mature uninfected leaves of *ntaq1* and *prt6* compared to WT (Figure 4, Supporting Information Fig. S6), including *PAD3*

(CYP71B15), that catalyzes the final two steps of camalexin synthesis. Interestingly, during a time-course following infiltration with *Pst* DC3000, levels of camalexin-associated transcripts, including *GSTF6* and *PAD3*, as well as *GSTF7* increased in WT but to a lesser extent in mutant leaves (Figure 4). Whilst basal levels of camalexin in uninfected leaves were similar in mutants and WT they increased to a greater degree in mutants than WT in response to infection (Figure 4). Mutant plants showed greater basal levels of indole-3-carboxylic acid (I3CA), a compound synthesized during the defence response and a potential precursor of camalexin through the action of GH3.5 (Forcat *et al.*, 2010; Wang *et al.*, 2012) that was also upregulated at the RNA level in untreated leaves of *ntaq1-3* (Figure 4). Camalexin synthesis is highly interconnected with other pathways of secondary metabolism, for example it has been reported that *vte2* and *cyp83a1*, mutants of key steps of tocopherol and aliphatic glucosinolate synthesis pathways respectively, show increased levels of camalexin (Sattler *et al.*, 2006; Liu *et al.*, 2016). *VTE2* and *CYP83A1* showed decreased expression in *ntaq1-3* and *prt6-1* in both basal and infected conditions (Figure 4, Supporting Information Fig. S8). Combination of a null *pad3* allele with *prt6-1* resulted in a loss of the *prt6* enhanced resistance to injected *Pst* DC3000 (Figure 5).

The Arg/N-end rule pathway regulates an age-dependent primed state in uninfected plants

Previous work showed that hypoxia-associated genes are ectopically up-regulated in *prt6* and *ate1 ate2* mutant seedlings (Gibbs *et al.*, 2011; Licausi, 2013). However, it was recently shown that this is age-dependent, that in mature mutant plants these genes are not up-regulated (Giuntoli *et al.*, 2017). We also observe a large reduction in expression of hypoxia genes in older *prt6* plants and saw a similar trend in WT for some genes (Supporting Information Fig. S9a). No age-related differences were found in *NTAQ1* expression in either WT or *prt6* backgrounds (Supporting Information Fig. S9B), however *GSTF6/7* and *PAD3* showed increased expression with age in *prt6-1* and *ntaq1-3* plants compared to WT (Figure 6a). In N-end rule mutants, compared to WT we found age-related increases for the SA responsive PATHOGENESIS RELATED (PR) protein genes *PR1* and *PR5*, while JA and ET responsive *PR3* and *PR4* showed no differences (Figure 6b). In barley, constitutive increase in expression of the SA-responsive genes *HvPR1* and *Hvß1-3 glucanase* (Horvath *et al.*, 2003; Rostoks *et al.*, 2003) was found in leaves of *HvPRT6* RNAi plants, and infection with *Bgh* did not result in an increase in expression in *HvPRT6* RNAi plants, that was observed in WT plants (Figure 6b).

Discussion

We show here that a role for Arg/N-end rule pathway-mediated immunity is conserved in flowering plants. In Arabidopsis we demonstrate physiological, biochemical and molecular roles for N-end rule component NTAQ1 in influencing basal defence by enhancing expression of defense proteins and synthesis of camelaxin, and a role for the ERFVII known substrates in influencing stomatal response, against the hemi-biotroph *Pst.* We show a role in barley of the Arg/N-end rule in response to the biotroph *Bgh* and hemi-biotroph *Ps japonica*. We suggest that benefits of increased immunity may not be realized against necrotrophic pathogens (as shown in the interaction between *Fusarium* spp. and barley). It has been documented that camalexin is part of the defence response against the necrotroph fungus *Botrytis cinerea*, inhibiting its growth in a dose-dependent manner (Ferrari *et al.*, 2003). In our experiments, there were no differences in responses of WT and *prt6* to *Botrytis cinerea* suggesting that independently of other mechanisms activated, an increase in camalexin in *prt6* may not reach a level necessary for reduction in fungal growth. A recent report showed N-end rule mutants, including alleles of *prt6*, *ate1 ate2* and *ntaq1* to be in general equal or more sensitive than WT Arabidopsis to a wide range of bacterial and fungal pathogens with diverse infection strategies and lifestyles (de Marchi *et al.*, 2016). Our results, in which plants were grown under either neutral days or under the short-day condition used by de Marchi *et al.*, showed opposite results (of increased resistance). Our results provide a consistent pattern across different levels of expression (including enhanced defence gene transcripts and increased levels of camalexin synthesis proteins in untreated plants, and consistent phenotypes between Arabidopsis and barley) that indicate a role for NTAQ1 substrates and ERFVIIs as component of the immune response that enhance resistance. Therefore, differences in observed phenotypes of N-end rule mutants in response to infection between our studies remain to be resolved.

A specific effect for ERFVIIs was observed in the stomatal response to *Pst*. ABA is an important component of stomatal response to pathogens (McLachlan *et al.*, 2014) and stabilized ERFVIIs enhance ABA sensitivity of stomata (Vicente *et al.*, 2017). We observed a large increase in stability of artificial Nt-Cys reporters in both Arabidopsis and barley. Stabilisation could be caused by shielding of the Nt, or a reduction of either NO or oxygen. We did not observe an increase in hypoxia-related gene expression (of *ADH1*) at the same time as GUS stabilization, however we did observe a decline in NR activity. Seemingly contradictory to this assertion is the well-

known burst of NO in response to *Pst* infection (Delledonne *et al.*, 1998). However, this burst occurs early following infection, well before the reduction in NR activity and stabilization of artificial Nt-Cys reporters in both Arabidopsis and barley. It has previously been shown that in the NR null mutant *nia1 nia2*, that produces very low NO levels, the NO burst in response to infection is highly reduced (Modolo *et al.*, 2006; Chen *et al.*, 2014). Further experiments would be required to determine a causative role of reduced NR activity leading to enhanced stabilization. Regardless of the mechanism of stabilization, the observation of increased stability of Nt-Cys substrates following infection in both Arabidopsis and barley indicates a conserved role for modulation of the Cys-Arg/N-end rule pathway, and function for Nt-Cys substrates, in response to pathogen infection that deserves further investigation. Enhanced ABA sensitivity and stomatal response to *Pst* of the *ntaq1* mutant also suggests that Nt-Gln substrate(s) contribute to the stomatal ABA response to pathogens, and explains why *erfVII* is more sensitive to *Pst* than *prt6 erfVII* (where NTAQ1 substrates are still stabilized). An opposite effect of ERFVIIs was shown for interactions of Arabidopsis with the biotroph *P. brassicae*, as ERFVIIs enhanced infection indirectly by influencing fermentation (Gravot *et al.*, 2016). These observations and others (Gibbs *et al.*, 2015), indicate an important role for ERFVIIs in the plant immune response.

Analysis of the response to *Pst* DC3000 *hrpA*$^-$, together with increased expression of SA-associated defence genes and increased camalexin synthesis, suggests a role for NTAQ1 in the onset of general and inducible PTI defence. An age-related increase in SA-related defence gene expression in N-end rule mutants was not matched by increased SA levels. This suggests a possible role for immune-related MAPK cascade activating MPK3/6 that are sufficient for SA-independent induction of most SA-responsive genes, including *PR1* (Asai *et al.*, 2002); concomitantly, it has been demonstrated that MPK3 and MPK6 activation triggers GSTF6, 7 (and DJ1E) protein accumulation, that produces an increase in camalexin (Xu *et al.*, 2008; Su *et al.*, 2011). The observed increased accumulation of camalexin in *ntaq1* and *prt6* provides one explanation for increased resistance of these mutants. Although expression of camalexin synthesis genes was ectopically upregulated in uninfected mature leaves of mutants, enhanced camalexin accumulation was only observed in response to infection. This may be the result of shunting of intermediate(s) to other secondary metabolism pathways. In line with this, unchallenged *ntaq1* and *prt6* plants show greater levels of I3CA**.** The observation that mutation of *pad3* reverts the enhanced resistance of *prt6* highlights the role of N-end rule regulated camalexin synthesis in enhancing the immune response.

How might NTAQ1 function during development and in response to pathogen attack? *NTAQ1* and *PRT6* expression do not change in response to pathogen attack. NTAQ1 function influences defence gene expression and synthesis of camalexin. We demonstrate that downstream responses to NTAQ1, measured as responsive gene expression, are modified during development (though the expression of *NTAQ1* (and *PRT6*) transcripts were not affected by aging) suggesting that NTAQ1 substrate(s) may show an age-dependent increase in abundance. Following protease cleavage their activity would be revealed in the *ntaq1* mutant, where they would remain ectopically stabilized. Following protease cleavage to reveal Nt-Gln NTAQ1 substrates should be degraded in WT plants. In this case, in mature WT leaves down-regulation of NTAQ1-linked protease activity (or NTAQ1 activity) in response to pathogen attack could result in substrate stabilization. Stabilized NTAQ1 substrate(s) (or uncleaved protease targets that provide substrates) may then function to enhance gene expression associated with defence genes and camalexin synthesis, both resulting in an enhanced basal immune response.

Our data support a conserved role of the Arg/N-end rule pathway in influencing plant immune responses. Barley contains one *NTAQ1* gene (MLOC_70886) (Mayer *et al.*, 2012). Manipulation of expression or activity of this gene will be required to understand whether an NTAQ1 activity is also required in defence in barley. An important goal of future work will be to identify Nt-Gln substrates that influence the immune response. Although NTAQ1-related genes are present in all major groups of eukaryotes, only a single example exists of a biochemical role for this enzyme and an associated substrate (Usp1) (Piatkov *et al.*, 2012). There is already evidence for Nt-Gln-bearing peptide fragments derived from proteins of diverse functions present in the plant METACASPASE-9 degradome (Tsiatsiani *et al.*, 2013), suggesting that substrates for NTAQ1 exist. Our results establish new components of the plant immune response, and offer new targets to enhance resistance against plant pathogens.

Acknowledgements: We thank Yin Yang and Daniel Beech (Nottingham) and Nancy De Winne (VIB, Gent) for technical assistance. This work was supported by the Biotechnology and Biological Sciences Research Council [grant numbers BB/K000144/1, BB/M029441/1, BB/K000063/1] (all including financial support from SABMiller plc), DR by a BBSRC DTP PhD fellowship, GMM by a Barry Axcell Fellowship, ND by a grants of the *ScienceCampus Halle – Plant-based Bioeconomy*

for setting up a junior research group, the Leibniz Association, and the Leibniz Institute of Plant Biochemistry (IPB); CN by a PhD fellowship of the Landesgraduiertenförderung Sachsen-Anhalt and the Deutsche Forschungsgemeinschaft (DFG) Graduate Training Center GRK1026 "*Conformational Transitions in Macromolecular Interactions*", CC and YI were supported by Spanish Ministry of Economy and Competitiveness grant BIO2015-68130. Work in A.B.'s laboratory was supported by ERA-Caps project N-vironment (Austrian Science Fund I1464-B16). VP was supported by Pla de formació Universitat Jaume I PI-1B2015-33 and the Instrumental Service of the University Jaume I SCIC.

Author contributions:

J.V, G.M.M, K.S, C.N., N.D, D.J.G, R.R, C.C, A.B, J.E.G, K.G, M.J.H Designed research; J.V, G.M.M, J.P, V.P, Y.I, C.N, D.R, M.M., R.R, A.B Performed research; J.V, G.M.M, R.R, N.D, C.C, M.J.H Analyzed data; J.V, M.J.H wrote the manuscript.

References:

Abbas M, Berckhan S, Rooney DJ, Gibbs DJ, Conde JV, Correia CS, Bassel GW, Marin-de la Rosa N, Leon J, Alabadi D, et al. 2015. Oxygen Sensing Coordinates Photomorphogenesis to Facilitate Seedling Survival. *Current Biology* **25**(11): 1483-1488.

Ajigboye OO, Bousquet L, Murchie EH, Ray RV. 2016. Chlorophyll fluorescence parameters allow the rapid detection and differentiation of plant responses in three different wheat pathosystems. *Functional Plant Biology* **43**(4): 356-369.

Arnaud D, Hwang I. 2015. A Sophisticated Network of Signaling Pathways Regulates Stomatal Defenses to Bacterial Pathogens. *Molecular Plant* **8**(4): 566-581.

Asai T, Tena G, Plotnikova J, Willmann MR, Chiu WL, Gomez-Gomez L, Boller T, Ausubel FM, Sheen J. 2002. MAP kinase signalling cascade in Arabidopsis innate immunity. *Nature* **415**(6875): 977-983.

Boller T, Felix G. 2009. A renaissance of elicitors: perception of microbe-associated molecular patterns and danger signals by pattern-recognition receptors. *Annu Rev Plant Biol* **60**: 379-406.

Chater C, Kamisugi Y, Movahedi M, Fleming A, Cuming AC, Gray JE, Beerling DJ. 2011. Regulatory Mechanism Controlling Stomatal Behavior Conserved across 400 Million Years of Land Plant Evolution. *Current Biology* **21**(12): 1025-1029.

Chen J, Vandelle E, Bellin D, Delledonne M. 2014. Detection and function of nitric oxide during the hypersensitive response in Arabidopsis thaliana: where there's a will there's a way. *Nitric Oxide* **43**: 81-88.

Clough SJ, Bent AF. 1998. Floral dip: a simplified method for *Agrobacterium*-mediated transformation of *Arabidopsis* thaliana. *Plant Journal* **16**(6): 735-743.

Dangl JL, Jones JD. 2001. Plant pathogens and integrated defence responses to infection. *Nature* **411**(6839): 826-833.

Davies RT, Goetz DH, Lasswell J, Anderson MN, Bartel B. 1999. IAR3 encodes an auxin conjugate hydrolase from Arabidopsis. *Plant Cell* **11**(3): 365-376.

de Marchi R, Sorel M, Mooney B, Fudal I, Goslin K, Kwasniewska K, Ryan PT, Pfalz M, Kroymann J, Pollmann S, et al. 2016. The N-end rule pathway regulates pathogen responses in plants. *Scientific Reports* **6**.

Delledonne M, Xia Y, Dixon RA, Lamb C. 1998. Nitric oxide functions as a signal in plant disease resistance. *Nature* **394**(6693): 585-588.

Dey S, Wenig M, Langen G, Sharma S, Kugler KG, Knappe C, Hause B, Bichlmeier M, Babaeizad V, Imani J, et al. 2014. Bacteria-Triggered Systemic Immunity in Barley Is Associated with WRKY and ETHYLENE RESPONSIVE FACTORs But Not with Salicylic Acid. *Plant Physiology* **166**(4): 2133-U1438.

Ferrari S, Plotnikova JM, De Lorenzo G, Ausubel FM. 2003. Arabidopsis local resistance to *Botrytis cinerea* involves salicylic acid and camalexin and requires EDS4 and PAD2, but not SID2, EDS5 or PAD4. *Plant J* **35**(2): 193-205.

Forcat S, Bennett M, Grant M, Mansfield JW. 2010. Rapid linkage of indole carboxylic acid to the plant cell wall identified as a component of basal defence in Arabidopsis against hrp mutant bacteria. *Phytochemistry* **71**(8-9): 870-876.

Gamir J, Pastor V, Cerezo M, Flors V. 2012. Identification of indole-3-carboxylic acid as mediator of priming against Plectosphaerella cucumerina. *Plant Physiology and Biochemistry* **61**: 169-179.

Gibbs DJ, Bacardit J, Bachmair A, Holdsworth MJ. 2014a. The eukaryotic N-end rule pathway: conserved mechanisms and diverse functions. *Trends in Cell Biology* **24**: 603–611.

Gibbs DJ, Conde JV, Berckhan S, Prasad G, Mendiondo GM, Holdsworth MJ. 2015. Group VII Ethylene Response Factors Coordinate Oxygen and Nitric Oxide Signal Transduction and Stress Responses in Plants. *Plant Physiology* **169**(1): 23-31.

Gibbs DJ, Isa NM, Movahedi M, Lozano-Juste J, Mendiondo GM, Berckhan S, Marin-de la Rosa N, Conde JV, Correia CS, Pearce SP, et al. 2014b. Nitric Oxide Sensing in Plants Is Mediated by Proteolytic Control of Group VII ERF Transcription Factors. *Molecular Cell* **53**(3): 369-379.

Gibbs DJ, Lee SC, Isa NM, Gramuglia S, Fukao T, Bassel GW, Sousa Correia C, Corbineau F, Theodoulou FL, Bailey-Serres J, et al. 2011. Homeostatic response to hypoxia is regulated by the N-end rule pathway in plants. *Nature* **479**: 415–418.

Giuntoli B, Shukla V, Maggiorelli F, Giorgi FM, Lombardi L, Perata P, Licausi F. 2017. Age-dependent regulation of ERF-VII transcription factor activity in Arabidopsis thaliana. *Plant Cell and Environment* **40**(10): 2333-2346.

Glazebrook J, Ausubel FM. 1994. Isolation of phytoalexin-deficient mutants of Arabidopsis thaliana and characterization of their interactions with bacterial pathogens. *Proceedings of the National Academy of Sciences of the United States of America* **91**(19): 8955-8959.

Graciet E, Mesiti F, Wellmer F. 2010. Structure and evolutionary conservation of the plant N-end rule pathway. *Plant Journal* **61**(5): 741-751.

Grant MR, Jones JDG. 2009. Hormone (Dis)harmony Moulds Plant Health and Disease. *Science* **324**(5928): 750-752.

Gravot A, Richard G, Lime T, Lemarié S, Jubault M, Lariagon C, Lemoine J, Vicente J, Robert-Seilaniantz A, Holdsworth MJ, et al. 2016. Hypoxia response in Arabidopsis roots infected by Plasmodiophora brassicae supports the development of clubroot. *Bmc Plant Biology* **16**(1): 251.

Grigoryev S, Stewart AE, Kwon YT, Arfin SM, Bradshaw RA, Jenkins NA, Copeland NG, Varshavsky A. 1996. A mouse amidase specific for N-terminal asparagine - The gene, the enzyme, and their function in the N-end rule pathway. *Journal of Biological Chemistry* **271**(45): 28521-28532.

Horvath H, Rostoks N, Brueggeman R, Steffenson B, von Wettstein D, Kleinhofs A. 2003. Genetically engineered stem rust resistance in barley using the Rpg1 gene. *Proceedings of the National Academy of Sciences of the United States of America* **100**(1): 364-369.

Hu RG, Sheng J, Qi X, Xu ZM, Takahashi TT, Varshavsky A. 2005. The N-end rule pathway as a nitric oxide sensor controlling the levels of multiple regulators. *Nature* **437**(7061): 981-986.

Kaiser JJ, Lewis OAM. 1984. Nitrate reductase and glutamine-synthetase activity in leaves and roots of nitrate-fed *Helianthus-annuus* L. *Plant and Soil* **77**(1): 127-130.

Karimi M, Bleys A, Vanderhaeghen R, Hilson P. 2007. Building blocks for plant gene assembly. *Plant Physiology* **145**(4): 1183-1191.

Lehmeyer M, Kanofsky K, Hanko EK, Ahrendt S, Wehrs M, Machens F, Hehl R. 2016. Functional dissection of a strong and specific microbe-associated molecular pattern-responsive synthetic promoter. *Plant Biotechnol J* **14**(1): 61-71.

Licausi F. 2013. Molecular elements of low-oxygen signaling in plants. *Physiologia Plantarum* **148**(1): 1-8.

Licausi F, Kosmacz M, Weits DA, Giuntoli B, Giorgi FM, Voesenek LACJ, Perata P, van Dongen JT. 2011. Oxygen sensing in plants is mediated by an N-end rule pathway for protein destabilization. *Nature* **479**: 419–422.

682 **Liu S, Bartnikas LM, Volko SM, Ausubel FM, Tang D. 2016.** Mutation of the
683 Glucosinolate Biosynthesis Enzyme Cytochrome P450 83A1 Monooxygenase
684 Increases Camalexin Accumulation and Powdery Mildew Resistance. *Front*
685 *Plant Sci* **7**: 227.
686 **Mayer KFX, Waugh R, Langridge P, Close TJ, Wise RP, Graner A, Matsumoto T,**
687 **Sato K, Schulman A, Muehlbauer GJ, et al. 2012.** A physical, genetic and
688 functional sequence assembly of the barley genome. *Nature* **491**(7426): 711-
689 716.
690 **McAinsh MR, Brownlee C, Hetherington AM. 1991.** PARTIAL INHIBITION OF
691 ABA-INDUCED STOMATAL CLOSURE BY CALCIUM-CHANNEL
692 BLOCKERS. *Proceedings of the Royal Society B-Biological Sciences*
693 **243**(1308): 195-201.
694 **McLachlan DH, Kopischke M, Robatzek S. 2014.** Gate control: guard cell
695 regulation by microbial stress. *New Phytol* **203**(4): 1049-1063.
696 **Mendiondo GM, Gibbs DJ, Szurman-Zubrzycka M, Korn A, Marquez J, Szarejko**
697 **I, Maluszynski M, King J, Axcell B, Smart K, et al. 2016.** Enhanced
698 waterlogging tolerance in barley by manipulation of expression of the N-end
699 rule pathway E3 ligase PROTEOLYSIS6. *Plant Biotechnology Journal* **14**(1):
700 40–50.
701 **Modolo LV, Augusto O, Almeida IMG, Pinto-Maglio CAF, Oliveira HC, Seligman**
702 **K, Salgado I. 2006.** Decreased arginine and nitrite levels in nitrate reductase-
703 deficient Arabidopsis thaliana plants impair nitric oxide synthesis and the
704 hypersensitive response to Pseudomonas syringae. *Plant Science* **171**(1): 34-
705 40.
706 **Moreno JI, Martin R, Castresana C. 2005.** Arabidopsis SHMT1, a serine
707 hydroxymethyltransferase that functions in the photorespiratory pathway
708 influences resistance to biotic and abiotic stress. *Plant Journal* **41**(3): 451-
709 463.
710 **Nawrath C, Metraux JP. 1999.** Salicylic acid induction-deficient mutants of
711 Arabidopsis express PR-2 and PR-5 and accumulate high levels of camalexin
712 after pathogen inoculation. *Plant Cell* **11**(8): 1393-1404.
713 **Park BS, Song JT, Seo HS. 2011.** Arabidopsis nitrate reductase activity is
714 stimulated by the E3 SUMO ligase AtSIZ1. *Nature Communications* **2**.
715 **Piatkov KI, Colnaghi L, Bekes M, Varshavsky A, Huang TT. 2012.** The Auto-
716 Generated Fragment of the Usp1 Deubiquitylase Is a Physiological Substrate
717 of the N-End Rule Pathway. *Molecular Cell* **48**(6): 926-933.
718 **Piatkov KI, Oh JH, Liu Y, Varshavsky A. 2014.** Calpain-generated natural protein
719 fragments as short-lived substrates of the N-end rule pathway. *Proceedings*
720 *of the National Academy of Sciences of the United States of America* **111**(9):
721 E817-E826.
722 **Pieterse CMJ, Leon-Reyes A, Van der Ent S, Van Wees SCM. 2009.** Networking
723 by small-molecule hormones in plant immunity. *Nature Chemical Biology* **5**(5):
724 308-316.
725 **Rostoks N, Schmierer D, Kudrna D, Kleinhofs A. 2003.** Barley putative
726 hypersensitive induced reaction genes: genetic mapping, sequence analyses
727 and differential expression in disease lesion mimic mutants. *Theoretical and*
728 *Applied Genetics* **107**(6): 1094-1101.
729 **Sánchez-Bel P, Sanmartín N, Pastor V, Mateu D, Cerezo M, Vidal-Albalat A,**
730 **Pastor-Fernández J, Pozo MJ, Flors V. 2018.** Mycorrhizal tomato plants fine
731 tunes the growth-defence balance upon N depleted root environments. *Plant,*
732 *Cell & Environment* **41**(2): 406-420.
733 **Sappl PG, Carroll AJ, Clifton R, Lister R, Whelan J, Millar AH, Singh KB. 2009.**
734 The Arabidopsis glutathione transferase gene family displays complex stress
735 regulation and co-silencing multiple genes results in altered metabolic
736 sensitivity to oxidative stress. *Plant Journal* **58**(1): 53-68.

Sattler SE, Mene-Saffrane L, Farmer EE, Krischke M, Mueller MJ, DellaPenna D. 2006. Nonenzymatic lipid peroxidation reprograms gene expression and activates defense markers in Arabidopsis tocopherol-deficient mutants. *Plant Cell* **18**(12): 3706-3720.

Schilling S, Stenzel I, von Bohlen A, Wermann M, Schulz K, Demuth HU, Wasternack C. 2007. Isolation and characterization of the glutaminyl cyclases from Solanum tuberosum and Arabidopsis thaliana: implications for physiological functions. *Biological Chemistry* **388**(2): 145-153.

Su T, Xu J, Li Y, Lei L, Zhao L, Yang H, Feng J, Liu G, Ren D. 2011. Glutathione-indole-3-acetonitrile is required for camalexin biosynthesis in Arabidopsis thaliana. *Plant Cell* **23**(1): 364-380.

Thao S, Zhao Q, Kimball T, Steffen E, Blommel PG, Riters M, Newman CS, Fox BG, Wrobel RL. 2005. Results from high-throughput DNA cloning of Arabidopsis thaliana target genes using site-specific recombination. *Journal of Structural and Functional Genomics* **5**(4): 267-276.

Thordal-Christensen H, Zhang ZG, Wei YD, Collinge DB. 1997. Subcellular localization of H_2O_2 in plants. H_2O_2 accumulation in papillae and hypersensitive response during the barley-powdery mildew interaction. *Plant Journal* **11**(6): 1187-1194.

Truman W, de Zabala MT, Grant M. 2006. Type III effectors orchestrate a complex interplay between transcriptional networks to modify basal defence responses during pathogenesis and resistance. *Plant J* **46**(1): 14-33.

Tsiatsiani L, Timmerman E, De Bock P-J, Vercammen D, Stael S, van de Cotte B, Staes A, Goethals M, Beunens T, Van Damme P, et al. 2013. The Arabidopsis METACASPASE9 Degradome. *Plant Cell* **25**(8): 2831-2847.

Varshavsky A. 2012. The Ubiquitin System, an Immense Realm. *Annual Review of Biochemistry* **81**: 167-176.

Vicente J, Mendiondo GM, Movahedi M, Peirats-Llobet M, Juan YT, Shen YY, Dambire C, Smart K, Rodriguez PL, Charng YY, et al. 2017. The Cys-Arg/N-End Rule Pathway Is a General Sensor of Abiotic Stress in Flowering Plants. *Current Biology* **27**(20): 3183-3190.

Vu LD, Stes E, Van Bel M, Nelissen H, Maddelein D, Inze D, Coppens F, Martens L, Gevaert K, De Smet I. 2016. Up-to-Date Workflow for Plant (Phospho)proteomics Identifies Differential Drought-Responsive Phosphorylation Events in Maize Leaves. *Journal of Proteome Research* **15**(12): 4304-4317.

Wang HQ, Piatkov KI, Brower CS, Varshavsky A. 2009. Glutamine-Specific N-Terminal Amidase, a Component of the N-End Rule Pathway. *Molecular Cell* **34**(6): 686-695.

Wang MY, Liu XT, Chen Y, Xu XJ, Yu B, Zhang SQ, Li Q, He ZH. 2012. Arabidopsis acetyl-amido synthetase GH3.5 involvement in camalexin biosynthesis through conjugation of indole-3-carboxylic acid and cysteine and upregulation of camalexin biosynthesis genes. *J Integr Plant Biol* **54**(7): 471-485.

Weits DA, Giuntoli B, Kosmacz M, Parlanti S, Hubberten HM, Riegler H, Hoefgen R, Perata P, van Dongen JT, Licausi F. 2014. Plant cysteine oxidases control the oxygen-dependent branch of the N-end-rule pathway. *Nature Communications* **5**: 3425.

White MD, Klecker M, Hopkinson RJ, Weits DA, Mueller C, Naumann C, O'Neill R, Wickens J, Yang JY, Brooks-Bartlett JC, et al. 2017. Plant cysteine oxidases are dioxygenases that directly enable arginyl transferase-catalysed arginylation of N-end rule targets. *Nature Communications* **8**.

Xu F, Huang Y, Li L, Gannon P, Linster E, Huber M, Kapos P, Bienvenut W, Polevoda B, Meinnel T, et al. 2015. Two N-Terminal Acetyltransferases

Antagonistically Regulate the Stability of a Nod-Like Receptor in Arabidopsis. *Plant Cell* **27**(5): 1547-1562.

Xu J, Li Y, Wang Y, Liu H, Lei L, Yang H, Liu G, Ren D. 2008. Activation of MAPK kinase 9 induces ethylene and camalexin biosynthesis and enhances sensitivity to salt stress in Arabidopsis. *J Biol Chem* **283**(40): 26996-27006.

Zhao J, Last RL. 1996. Coordinate regulation of the tryptophan biosynthetic pathway and indolic phytoalexin accumulation in Arabidopsis. *Plant Cell* **8**(12): 2235-2244.

Zhou BJ, Zeng LR. 2017. Conventional and unconventional ubiquitination in plant immunity. *Molecular Plant Pathology* **18**(9): 1313-1330.

Figure legends:

Figure 1: Genetic characterization of the role of the N-end rule pathway in the apoplastic response to *Pst* DC3000

a. Schematic of the Arg/N-end rule pathway. Single letter codes for residues are shown. PRT6; PROTEOLYSIS6, ATE; arginyl transferase, NTAN; Nt-Asn amidase, NTAQ; Nt-Gln amidase, PCO; PLANT CYSTEINE OXIDASE. Black ovals represent protein substrates.

b. Quantification of *Pst* DC3000 growth in WT and mutant plants 2 and 4 days after bacterial infiltration (10^6 cfu ml^{-1}).

c. Ion leakage measurement in leaves 4 days after infiltration with *Pst* DC3000 (10^7 cfu ml^{-1}).

d-f. Quantification of bacterial growth in WT and mutant plants 4 days after bacterial infiltration (10^6 cfu ml^{-1}).

g. Enzyme activity of bacterially produced NTAQ1 against peptides with different Nt-residues (- = GAGSW). Data represent means ± SEM. Statistical differences were analyzed by ANOVA followed by Tukey test ($P < 0.05$) or Student's t-test *p <0.05, **p < 0.01, ***p < 0.001.

Figure 2: Genetic characterization of the role of the N-end rule pathway in the stomatal response to *Pst* DC3000

a-d. Quantification of *Pst* DC3000 growth in WT and mutant plants 4 days after bacterial infiltration by injection (10^6 cfu ml^{-1}) or bacterial foliar spray application (10^8 cfu ml^{-1}).

c. Stomatal aperture response to applied *Pst* DC3000 in WT and mutants.

e. Total NR enzyme activity following foliar application of *Pst* DC3000 (10^8 cfu ml^{-1}).

f. Expression of *NIA1* and *NIA2* RNA following leaf infiltration with *Pst* DC3000.

g. Stabilisation of C-^{HA}GUS protein and expression of *MC-^{HA}GUS* and *ACTIN* RNA in WT Arabidopsis plants sprayed with *Pst* DC3000 (10^8 cfu ml^{-1}).

h. Stabilisation of C-^{HA}GUS 24h after injection with flg22 (1μM) or H_2O. CBB, Coomassie Brilliant Blue. Data represent means ± SEM. Statistical differences were analyzed by ANOVA followed by Tukey test ($P < 0.05$) or Student's t-test *p <0.05, **p < 0.01, ***p < 0.001.

Figure 3: Analysis of N-end rule function in barley

a. Quantification of *Ps* pv *japonica* growth in *HvPRT6* RNAi and WT (cv. Golden Promise) (null segregant from the same transformation event) plants 4 days after bacterial infiltration (10^8 cfu ml^{-1}).
b,c. Measurement of total and leaf area infected in WT and *HvPRT6* RNAi barley plants with *Blumeria graminis* f. sp. *hordei* (*Bgh*).
d. Necrotic lesions on WT and *HvPRT6* RNAi barley plants 5 days following inoculation with *Fusarium graminearum* or *F. culmorum*.
e. Stabilisation of CGGAIL-GUS and expression of *MCGGAIL-GUS* and *TUBULIN* RNA in barley following infection with *Ps* pv *japonica* (10^8 cfu ml^{-1}) (4 days) or *Bgh* (14 days). CBB, Coomassie Brilliant Blue. Data represent means ± SEM. Statistical differences were analyzed Student's t-test *p <0.05, **p < 0.01, ***p < 0.001.

Figure 4: Influence of NTAQ1 and PRT6 on camalexin and associated secondary metabolism in response to infiltration with *Pst* DC3000 (10^6 cfu ml^{-1}).
Schematic representation of the camalexin synthesis pathway highlighting time courses of changes in RNA expression (QrtPCR) or metabolites in WT, *ntaq1-3* or *prt6-1* in response to bacterial infection. IAOx, indole-3-acetaldoxime; IAN, indole-3-acetonitrile; GSH, glutathione; DHCA, dihydrocamalexin acid; IAA, indole-3-acetic acid; I3CA, indole-3-carboxilic acid; *GH3.5*, *IAA-AMIDO SYNTHASE*; *PAD3*, *PHYTOALEXIN DEFICIENT 3*. Data represent means ± SEM. Student's t-test *p <0.05, **p < 0.01, ***p<0.001.

Figure 5: Genetic interaction between *pad3* and *prt6* influences the apoplastic response to *Pst* DC3000.
Quantification of bacterial growth in WT and mutant plants 4 days after bacterial infiltration (10^6 cfu ml^{-1}). Data represent means ± SEM. Statistical differences were analyzed by ANOVA followed by Tukey test ($P < 0.05$).

Figure 6: Age-dependent priming of transcriptomic changes during development and defence.
a. Relative expression of genes of camalexin synthesis in WT and mutant plants.
b. Relative expression of transcripts encoding defence-related genes in WT and mutant plants.
c. Relative expression of *HvPR1* and *Hvβ1-3 glucanase* in WT and *HvPRT6* RNAi barley plants infected with *Blumeria graminis* f. sp. *hordei*.

874 Data represent means ± SEM. Statistical differences were analyzed by Student's t-
875 test *p <0.05, **p < 0.01, ***p < 0.001.
876
877

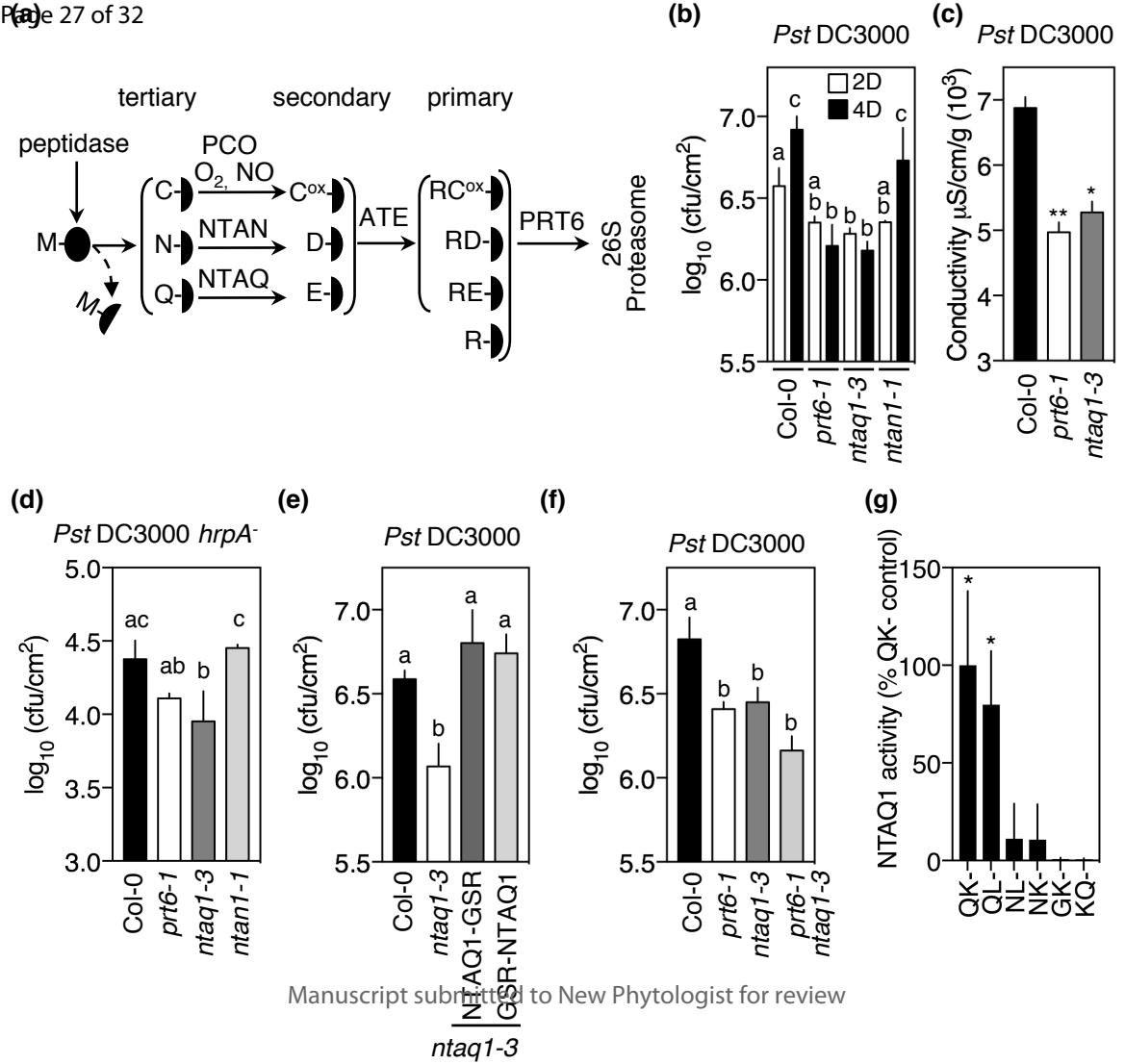
(a)
tertiary
secondary
primary
peptidase
PCO
O2, NO
C
N
Q
NTAN
NTAQ
Cox
D
E
ATE
RCox
RD
RE
R
PRT6
26S Proteasome
M
M-
(b)
Pst DC3000
2D
4D
log10 (cfu/cm2)
Col-0
prt6-1
ntaq1-3
ntan1-1
(c)
Pst DC3000
Conductivity µS/cm/g (10³)
Col-0
prt6-1
ntaq1-3
(d)
Pst DC3000 hrpA-
log10 (cfu/cm2)
Col-0
prt6-1
ntaq1-3
ntan1-1
(e)
Pst DC3000
log10 (cfu/cm2)
Col-0
ntaq1-3
NTAQ1-GSR
GSR-NTAQ1
ntaq1-3
(f)
Pst DC3000
log10 (cfu/cm2)
Col-0
prt6-1
ntaq1-3
prt6-1 ntaq1-3
(g)
NTAQ1 activity (% QK- control)
QK-
QL-
NL-
NK-
GK-
KQ-

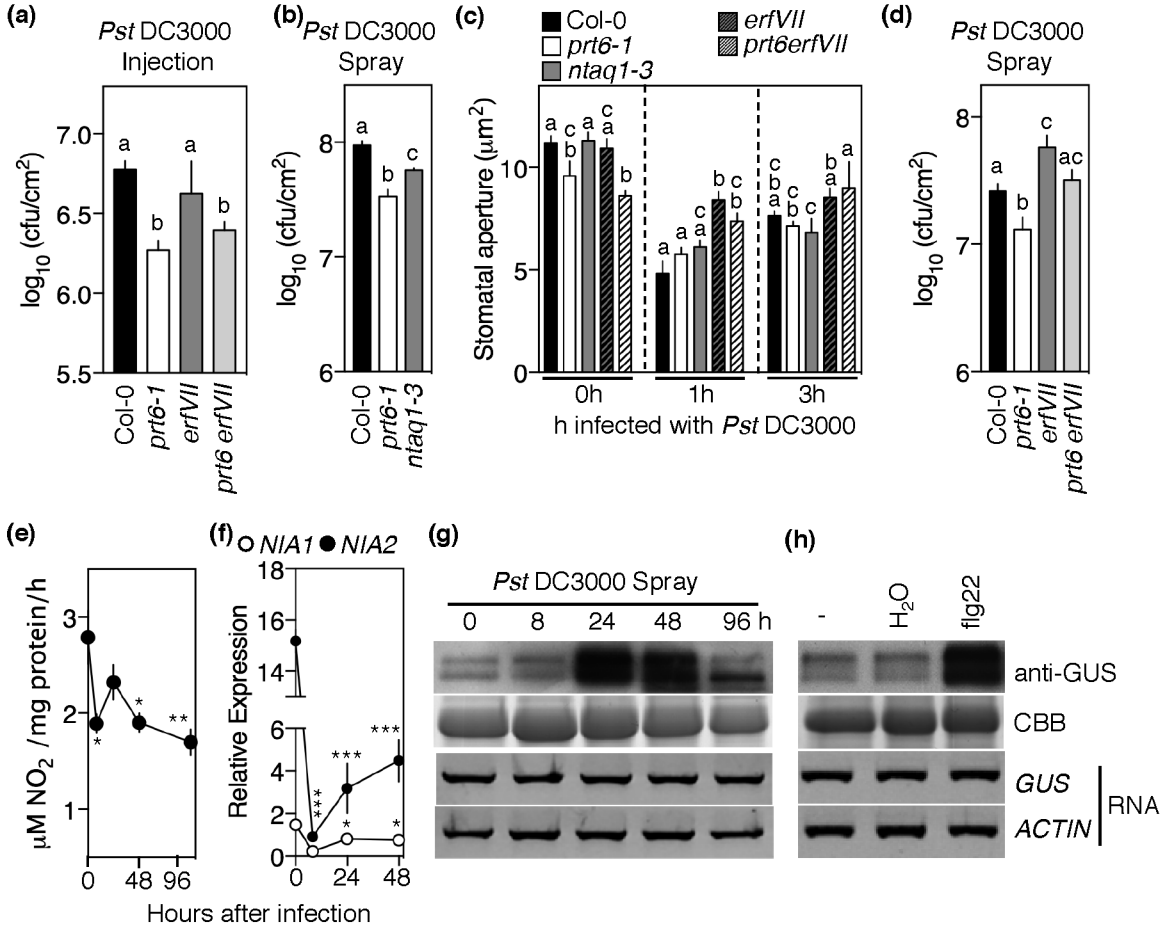
(a)
Pst DC3000
Injection
log10 (cfu/cm2)
Col-0
prt6-1
erfVII
prt6 erfVII
(b)
Pst DC3000
Spray
log10 (cfu/cm2)
Col-0
prt6-1
ntaq1-3
(c)
Col-0
prt6-1
ntaq1-3
erfVII
prt6erfVII
Stomatal aperture (µm2)
0h
1h
3h
h infected with Pst DC3000
(d)
Pst DC3000
Spray
log10 (cfu/cm2)
Col-0
prt6-1
erfVII
prt6 erfVII
(e)
µM NO2 /mg protein/h
Hours after infection
(f)
NIA1
NIA2
Relative Expression
(g)
Pst DC3000 Spray
0
8
24
48
96 h
(h)
-
H2O
flg22
anti-GUS
CBB
GUS
ACTIN
RNA

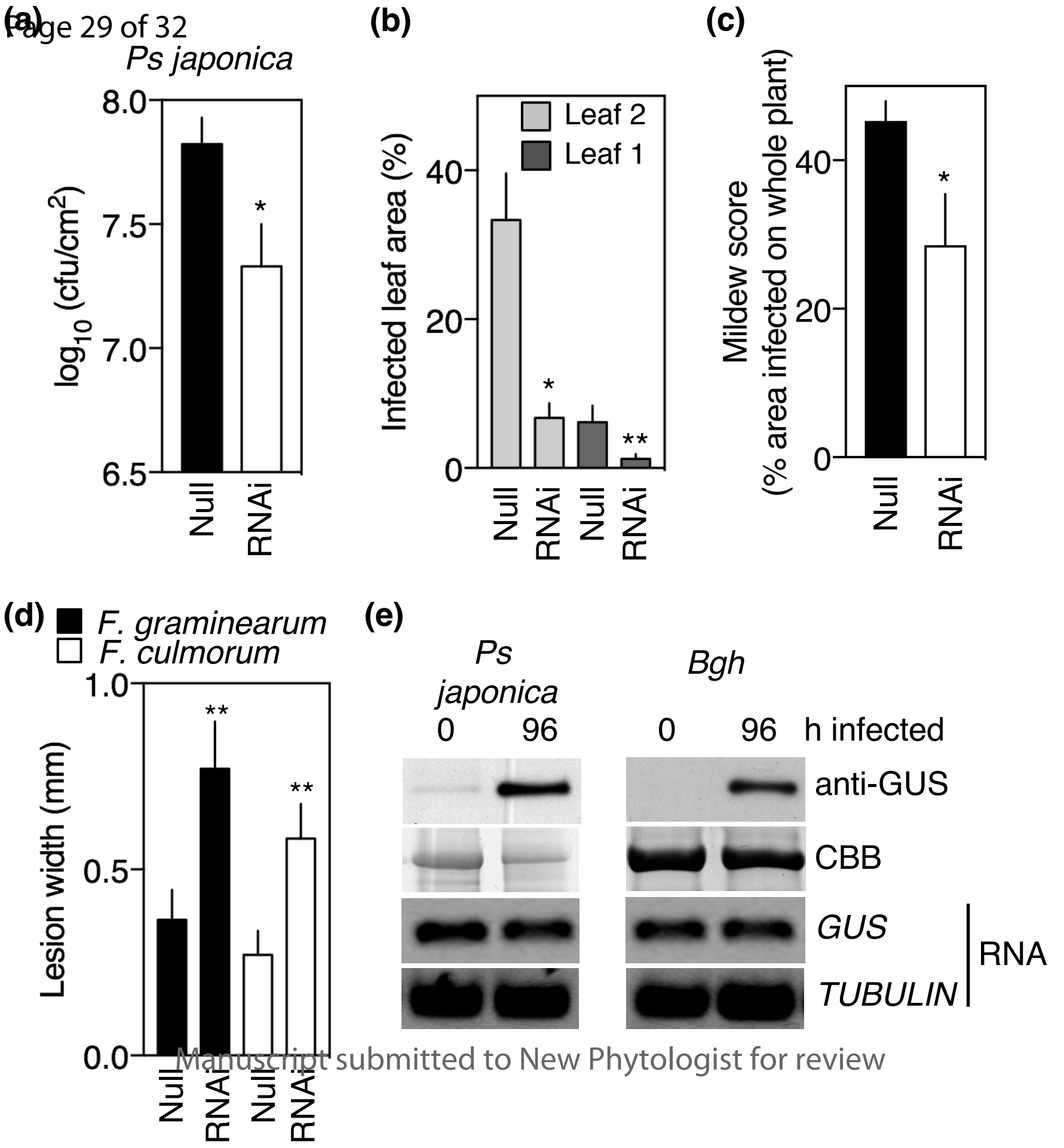

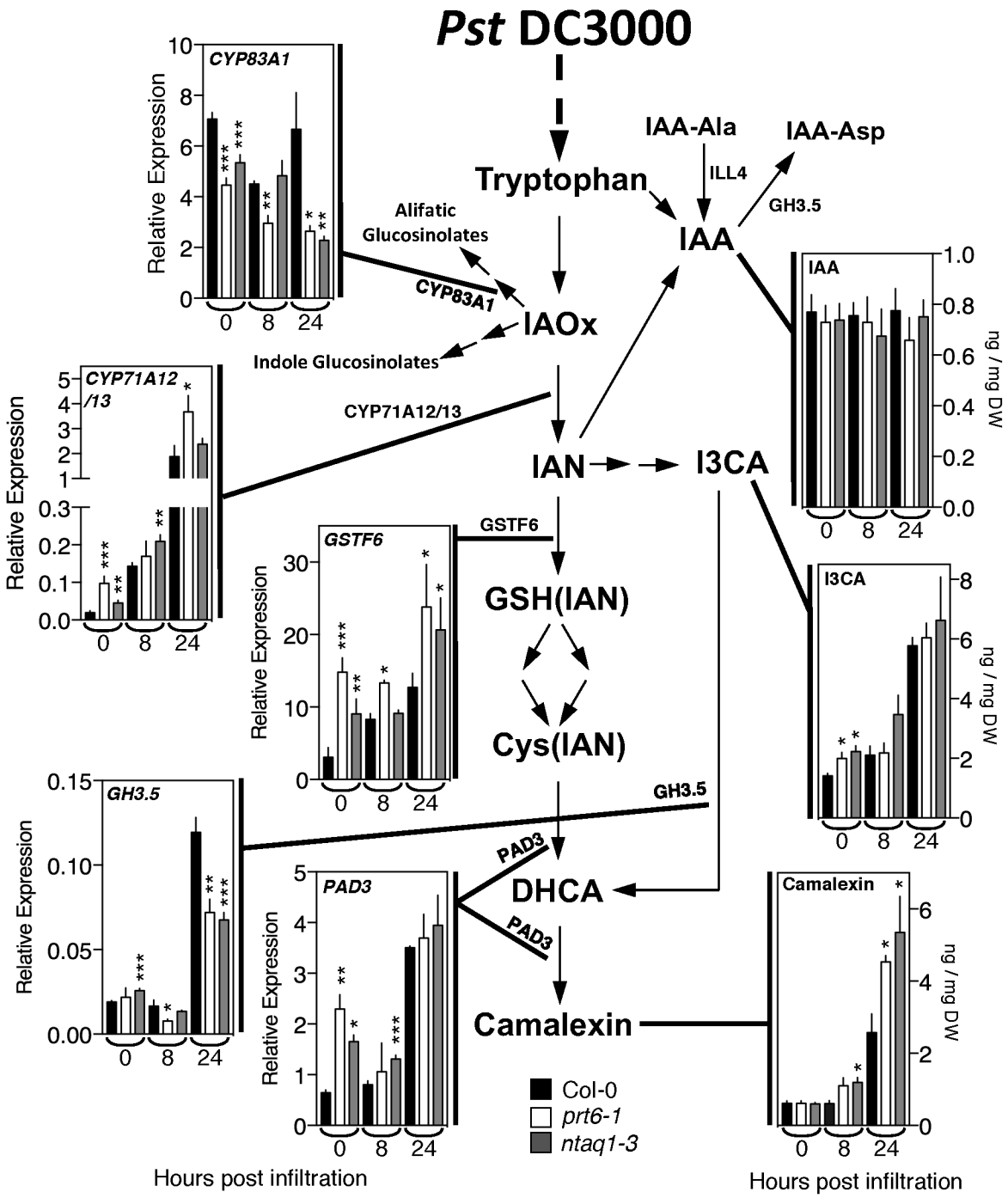
Pst DC3000
Tryptophan
IAA-Ala
IAA-Asp
ILL4
GH3.5
IAA
Alifatic Glucosinolates
CYP83A1
IAOx
Indole Glucosinolates
CYP71A12/13
IAN
I3CA
GSTF6
GSH(IAN)
Cys(IAN)
GH3.5
PAD3
DHCA
PAD3
Camalexin
CYP83A1
Relative Expression
IAA
ng / mg DW
CYP71A12 /13
GSTF6
I3CA
GH3.5
PAD3
Camalexin
Col-0
prt6-1
ntaq1-3
Hours post infiltration
Hours post infiltration

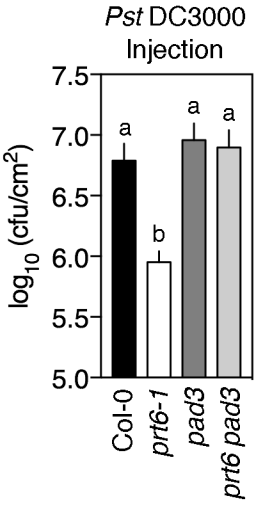
Pst DC3000
Injection
7.5
7.0
6.5
6.0
5.5
5.0
log10 (cfu/cm2)
a
b
a
a
Col-0
prt6-1
pad3
prt6 pad3

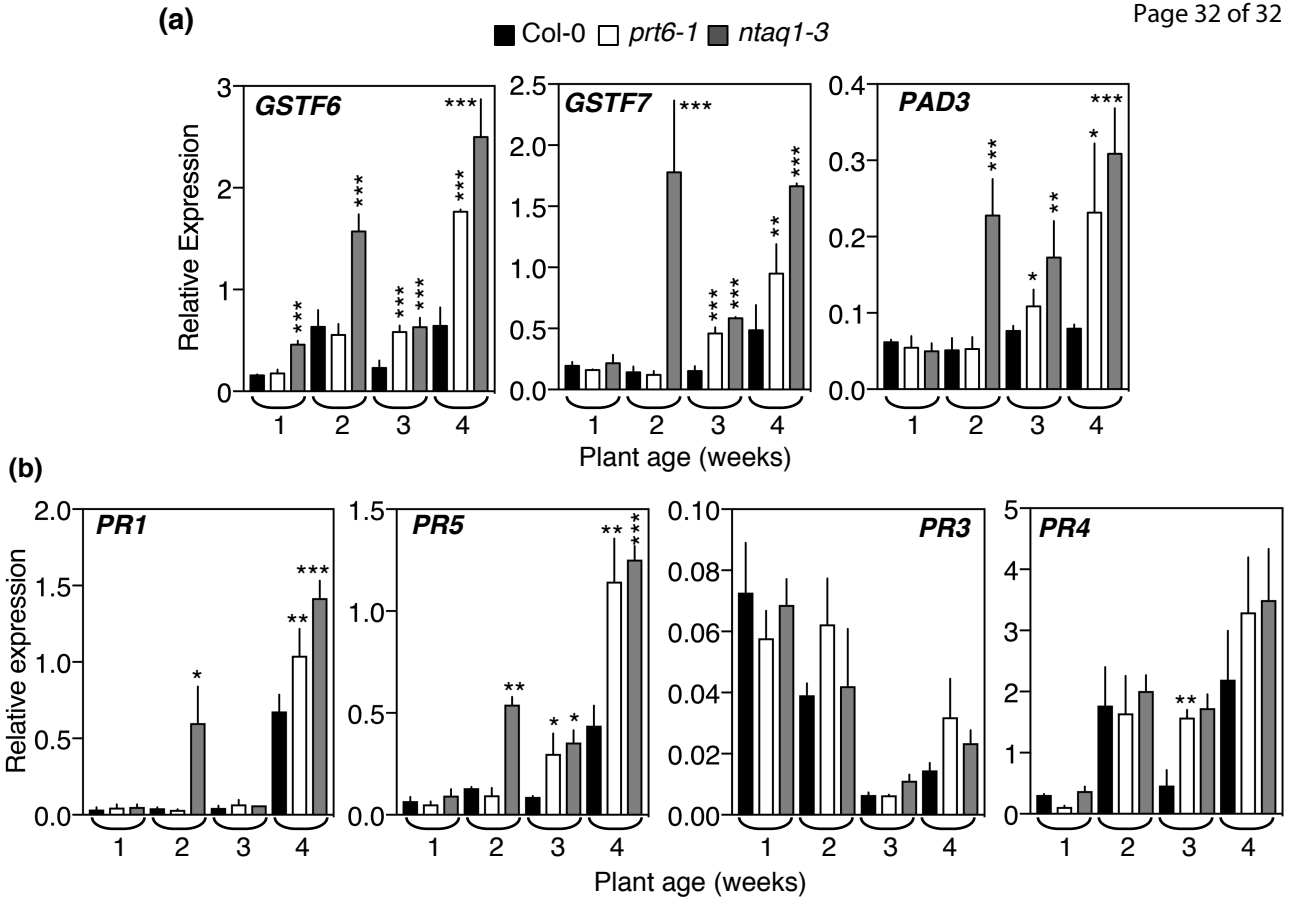
(a)
Col-0 prt6-1 ntaq1-3
GSTF6
GSTF7
PAD3
Relative Expression
Plant age (weeks)
(b)
PR1
PR5
PR3
PR4
Relative expression
Plant age (weeks)
(c)
h infected: 0 8 17
HvPR1
Hvβ1-3g
Relative expression
Null
RNAi